Talanta 116 (2013) 396–402

Contents lists available at ScienceDirect

Talanta

journal homepage: www.elsevier.com/locate/talanta

Preparation and application of surface molecularly imprinted silica gel for selective extraction of melamine from milk samples

Wenjing Cheng, Zhujuan Liu, Yan Wang *

Academy of Fundamental and Interdisciplinary Sciences, Harbin Institute of Technology, Harbin 150001, China

ARTICLE INFO

Article history:
Received 27 February 2013
Received in revised form
26 May 2013
Accepted 30 May 2013
Available online 5 June 2013

Keywords:
Molecularly imprinted polymer
Silica gel
Solid-phase extraction
Melamine

ABSTRACT

Highly selective molecularly imprinted layer-coated silica gel (MIP@SiO_2) for melamine (MEL) was prepared by the surface molecular imprinting technique on the supporter of silica gel. Non-imprinted polymer layer-coated silica gel (NIP@SiO_2) and bulk molecularly imprinted polymer (MIP) were also prepared for comparison. Characterization and performance tests of the obtained products revealed that MIP@SiO_2 not only had excellent selectivity to the target molecule MEL compared with NIP@SiO_2, but also displayed absorption capacity superior to MIP due to the molecular recognition sites on the surface of silica gel. As the MIP@SiO_2 were adopted as the adsorbents of solid-phase extraction for detecting MEL in milk samples, the recoveries of spiked samples ranged from 75.6% to 96.8% with the relative standard deviation of spiked samples less than 10%, which reveals that the MIP@SiO_2 were efficient SPE adsorbents for melamine.

© 2013 Elsevier B.V. All rights reserved.

1. Introduction

Melamine (2, 4, 6-Triamino-s-triazine, MEL) is an important chemical widely used in the production of melamine resins, which are used in laminates, glues, adhesives, and plastics [1,2]. Because of its wide dispersive use and toxic properties [3,4], monitoring of MEL has been giving rise to international concern. Generally, samples containing MEL are of complicated matrices, and MEL exists in very low concentration, so determination of MEL often requires effective sample preparation prior to instrumental analysis. Heretofore, solid-phase extraction (SPE) is the most used technique for the extraction of MEL from MEL-containing sample [5–11].

However, traditional SPE sorbents are short of selectivity for MEL in complex matrices, which makes the subsequent analysis of MEL very difficult. Recently, molecularly imprinted polymers (MIPs) for MEL have been used as SPE sorbents and seem to become the promising development to surround the drawbacks of traditional SPE sorbents owing to the higher recognition ability of MIPs for the given molecules [12–17].

In researches reported, most MIPs for MEL were prepared by bulk polymerization or precipitation polymerization [13–15,18]. As we know, these kinds of MIPs exhibit high selectivity but low rebinding capacity, poor site accessibility to target species and leakage of template molecules [19–21], because the imprinted polymer matrices are usually thick, and the template molecules are embedded in the matrices too deeply to be fully eluted [12]. In order to overcome these drawbacks effectively, the surface molecular imprinting technique has been developed [22–27]. With this technique, the disadvantages of traditional MIPs have been avoided to some extent. However, little attention has been paid to synthesize MIPs for MEL by the surface molecular imprinting technique.

Silica gel as a solid support is of great importance because it possesses some definite advantages, such as nondeforming, good mechanical strength and heat-stable [28]. Besides, the surface functionalization of silica gel to introduce additional functionality can be easily obtained by organosilicone.

Therefore, in this study, we reported highly selective core–shell molecularly imprinted polymers of MEL on the surface of silica gel (termed as MIP@SiO_2 hereafter). The Fourier transform infrared spectrometer (FT-IR), scanning electron microscope (SEM), thermogravimetric analysis (TGA) and nitrogen adsorption–desorption experiment shows that MIP@SiO_2 prepared successfully. The result of dynamic adsorption indicated that the prepared MIP@SiO_2 offered a fast kinetics for the rebinding of MEL. The high capacity to uptake MEL molecules showed that the effective imprinted sites in the MIP@SiO_2 were nearly 2-fold that of the NIP@SiO_2 and MIP. Meanwhile, the MIP@SiO_2 was successfully used as SPE materials coupled with HPLC to analyze trace amounts of MEL from the complex matrix samples.

2. Experimental

2.1. Reagents and materials

Silica gel, acetone, acetonitrile and methanol were purchased from Sinopharm Chemical Reagent Co., Ltd. Melamine (MEL) was

* Corresponding author. Tel.: +86 45186403719.
E-mail address: wangy_msn@hotmail.com (Y. Wang).

0039-9140/$ - see front matter © 2013 Elsevier B.V. All rights reserved.
http://dx.doi.org/10.1016/j.talanta.2013.05.067

purchased from Tianjin Kemiou Chemical Reagent Co., Ltd. Methacrylic acid (MAA) was purchased from Tianjin bodi Chemical Reagent Co., Ltd. Ethylene glycol dimethacrylate (EGDMA) was purchased from Aladdin Reagent Co., Ltd. 2,2′-Azobis (2-methylpropionitrile) (AIBN) was purchased from Tianjin Guangfu Fine Chemical institute. Vinyltrimethoxysilane (VTTS) were purchased from Nanjing Nengde Chemical Reagent Co., Ltd. Acetic acid, toluene, hydrochloric acid, glycol and pyridine were purchased from Tianjin Fuyu Fine Chemical Co., Ltd. All the reagents were of analytical grade. Water was doubly distilled. Pure milk and milk powder samples were purchased from a supermarket and stored at 277 K.

2.2. Fabrication procedure of MEL-imprinted silica (MIP@SiO_2)

Fabrication procedure of MEL-imprinted silica consisted of three steps as showed in Fig. 1, and the detailed descriptions were as follows:

(i) Activation of Silica gel. Silica gel (12 g) was dispersed in 100 mL of hydrochloric acid solution (10%) with stirring, and refluxed for 24 h under 385 K to increase the number of surface silanol. The product was filtered, washed with distilled water to neutral and dried at 393 K for 24 h.

(ii) Modification of silica gel with VTTS. 5 g Activated silica gel was dispersed in 100 mL toluene by ultrasound for 10 min, and then the solution was transferred into a three-necked flask, then VTTS (20 mL) was added. Amount of pyridine was added to maintain the acidity of the solution. The reaction was carried out at 398 K under nitrogen for 24 h. The product was filtered, washed with toluene and acetone to remove the unreacted reagent, and dried under vacuum for 24 h at 333 K.

(iii) Molecularly imprinting on the surface of VTTS–SiO_2. The obtained modified VTTS–SiO_2 was dispersed in 60 mL toluene by ultrasonic vibration. MEL (31.5 mg, 0.25 mmol) as the template, MAA (85 μL, 1 mmol) as the functional monomer, EGDMA (0.95 mL, 5 mmol) as the cross-linker and AIBN (30 mg) as the initiator were added and dissolved in the above solution. The polymerization reaction was carried out at 343 K under nitrogen for 24 h. The product was filtered, washed with a mixture of methanol and acetic acid (4:6, v/v) under ultrasonic vibration for 30 min. MEL was removed by Soxhlet extraction with the mixture of methanol and acetic acid (4:6, v/v) for 24 h, and then Soxhlet extraction with ethanol for 24 h. The product was filtered, washed

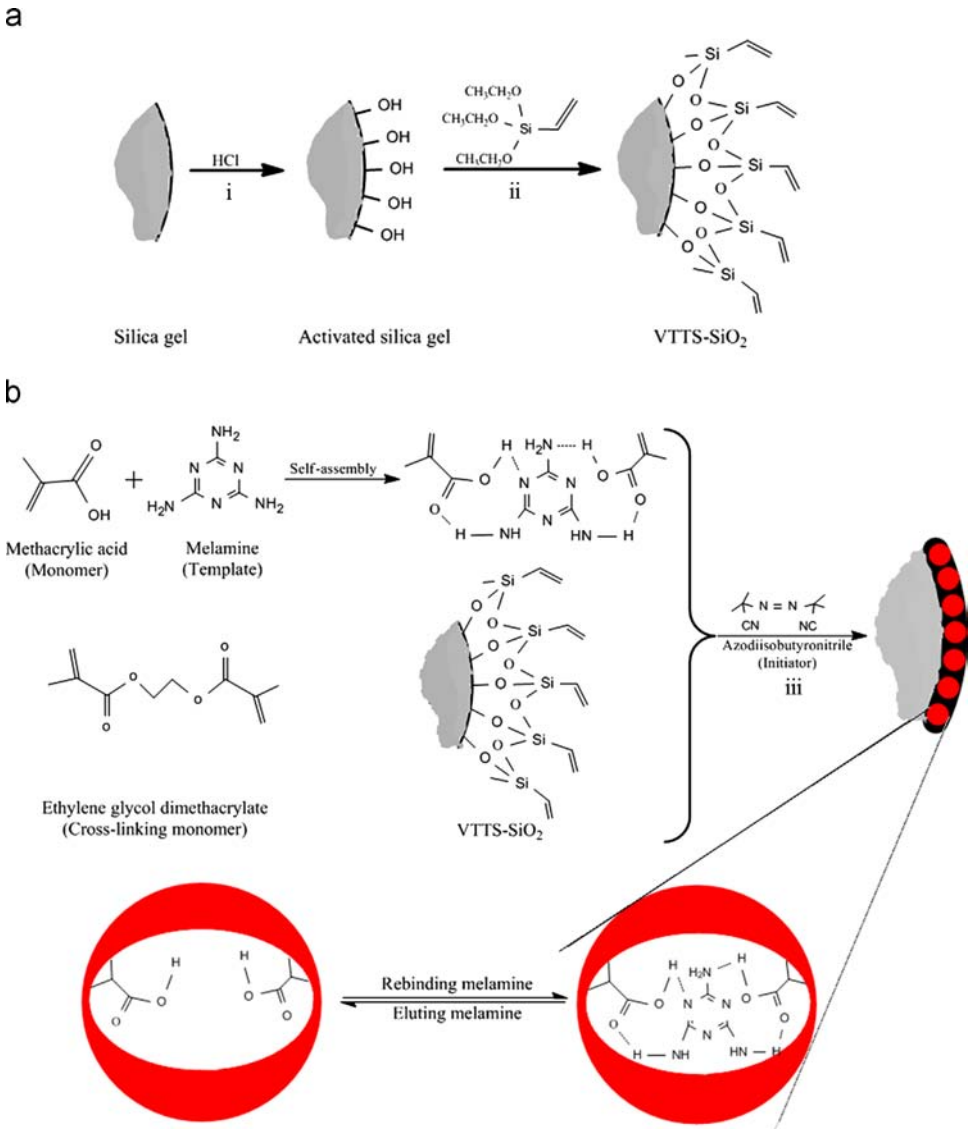

Fig. 1. Fabrication procedure of MIP@SiO_2.

with acetone and dried under vacuum for 24 h at room temperature.

The non-imprinted polymer (NIP@SiO_2) was fabricated identically but without the addition of template molecules. The bulk molecularly imprint polymer (MIP) was prepared the same as MIP@SiO_2 but without the support of silica gel (SiO_2).

2.3. Characterization and performance test of MIP–SiO_2

Scanning electron microscopy (SEM) images and energy dispersive spectroscopy were obtained on a Hitachi S-3000N microscope, with a voltage of 10.0 kv and a magnification of 200 and 20,000. Fourier transform infrared spectra (FTIR) were recorded on a Nicolet Avatar-360 instrument. Thermogravimetric (TG) and differential thermal (DTA) analyses were carried out simultaneously using a ZRY-2P instrument. Nitrogen adsorption was carried out on a Quantachrome Autosorb-1-c with a bath temperature of 77 K. Surface areas were determined using the Brunauer–Emmett–Teller (BET) theory, and pore size distributions were calculated using the Barrett–Joyner–Halenda (BJH) theory from the adsorption branch. UV/vis spectra were recorded on a TU-1800 UV/vis spectrophotometer.

The adsorption isotherms were obtained by suspending 10 mg MIP@SiO_2 in 4 mL glycol/acetonitrile solution (1:20, v/v) with different MEL concentrations (5–62.5 mg mL^{-1}). Meanwhile, the adsorption kinetic curves were obtained by detecting the temporal evolution of MEL concentration (10 mg L^{-1}) in the solutions. The binding amount of MEL on MIP@SiO_2 was determined by the difference between the total MEL amount and residual amount in the solution with TU-1800 the UV/vis spectrophotometer.

The adsorption capacity Q (mg/g) is calculated according to the equation as follows:

$$Q = \frac{(C_o - C_f)v}{m} \quad (1)$$

where C_o (mg/L) and C_f (mg/L) are the initial and final concentrations of MEL in solution, respectively, V (L) is the total volume of the solution, and m is the mass of MIP–SiO_2.

$$\frac{C_e}{Q} = \frac{C_e}{Q_{max}} + \frac{1}{KQ_{max}} \quad (2)$$

where Q and Q_{max} (mg/g) are the experimental and theoretical saturated adsorption capacities of MEL, respectively, C_e (mg/L) is the corresponding concentration of MEL in solution, and K (L/g) is the Langmuir adsorption equilibrium constant [29].

The competitive adsorption was evaluated among MEL and its structure analog tricyanicacid (CA) with three different concentrations (10, 22.5 and 62.5 mg L^{-1}). The repeatability was tested by detecting the spiked sample five times using the same MIP@SiO_2.

2.4. Determination of MEL in milk samples

All milk samples were pretreated before analysis by the following procedure. First, protein was removed from the matrix by adding acetonitrile (30 mL) to 10 mL milk or 10 g milk powder samples. After being shaken for 35 min and centrifuged for 10 min, the supernatant was collected to reserve.

HPLC (Agilent 1200) was used to determine the amount of MEL in milk samples. HPLC experimental conditions were as follows: the mobile phase was consisted of sodium 1-octanesulfonate solution/methanol (40:60, v/v), the pH value of mobile phase was adjust to 3 by phosphate buffer solution, the flow rate was maintained at 0.5 mL min^{-1}, the wavelength of ultraviolet detector was 240 nm. The method limit of detection (LOD) and limit of quantitation (LOQ) were defined as 3 and 10 times ratio of signal to noise, respectively.

2.5. Evaluation of MIP@SiO_2 as SPE sorbent for the analysis of milk samples

MIP@SiO_2 and NIP@SiO_2, each weighting 100 mg were dry-packed in an empty SPE cartridge between two glass wool frits, the obtained SPE cartridge termed as MI-SPE and NI-SPE, respectively. After activated by 4 mL water and 4 mL methanol, 1.0 mL of stock solution was loaded, and rinsed with 2 mL deionized water and 2 mL methanol. Then eluted with 2 mL the mixture of methanol and acetic acid (4:6, v/v), which was allowed to flow through, collected, evaporated to dryness, and redissolved in 1.0 mL of mobile phase.

3. Results and discussion

3.1. Characterization of the MIP@SiO_2

Fig. 2 shows the FT-IR spectra of activated silica gel particles, VTTS-SiO_2, MIP@SiO_2 and MIP. The bands at 1080 and 970 cm^{-1} were the characteristic vibration absorption of the Si–OH for the silica gel particles, and the band about 1640 cm^{-1} was the bending vibration of hydroxyl on the surface of silica gel. Since the position of characteristic peak for C=C group would be close to that of Si–OH at 1640 cm^{-1} and the intensity of C=C vibration was also very weak, therefore, comparing with silica gel, the IR spectrum of VTTS–SiO_2 did not show significant difference in Fig. 2(b). However, the following characterization of EDX and TGA can prove that VTTS was grafted on the surface of silica gel successfully. Strong peaks at 2970, 1730, 1460 and 1380 cm^{-1} appeared as shown in Fig. 2(c) and (d); 2970, 1460 and 1380 cm^{-1} were attributed to the stretching and bending vibration of methyl and methylene; the peak at 1730 cm^{-1} indicated the existence of the C=O group, indicating that MIP modified on the surface of silica gel. The bands in Fig. 2(c) were similar to Fig. 2(d), further demonstrating that MIP was grown on the surface of silica gel. Based on the above results, it can be known that the fabrication procedure (in Section 2) has been successfully performed.

Table 1 shows the data of energy-dispersive X-ray spectroscopy (EDX) with different samples. Carbon element appeared, suggesting that VTTS has been grafted on the surface of

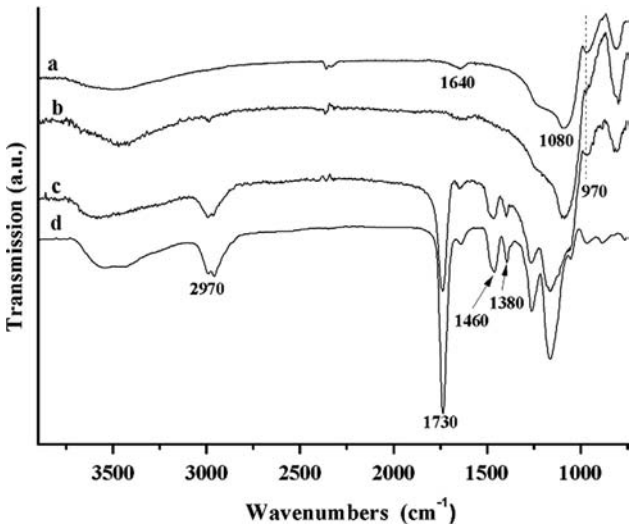

Fig. 2. FTIR spectra of activated silica gel particles (a), VTTS–SiO_2 (b), MIP@SiO_2 (c) and MIP (d).

silica gel. The relative content of C in the surface of MIP@SiO_2 was more than that of VTTS–SiO_2, which further proves that MIP grown on the surface of VTTS–SiO_2.

Fig. 3 shows the thermal decomposition pattern of silica gel, VTTS–SiO_2 and MIP@SiO_2. Silica gel had only one weight loss stage around 100 °C corresponding to the release of physically adsorbed water. VTTS–SiO_2 had three weight loss stage: first stage around 100 °C corresponding to the release of physically adsorbed water. Second stage around 280∼320 °C, which is rapid, corresponding to the degradation of VTTS silane coupling agent. And the slow 3rd stage around 320∼600 °C which corresponds to the decomposition of char formed in the second stage. The curve of MIP@SiO_2 is similar to VTTS–SiO_2, but the 2nd stage around 280∼400 °C, which is rapid, corresponding to the degradation of MIP, and the loss weight (38%) was much more than VTTS–SiO_2 (5.5%), further indicating that MIP grown on the surface of silica gel.

Table1
EDS element analysis of silica gel, VTTS–SiO_2 and MIP@SiO_2.

Relative content of element (%)	Silica gel	VTTS–SiO_2	MIP@SiO_2
C	0	19.88	80.34
O	30.67	21.88	16.26
Si	69.33	58.24	3.4

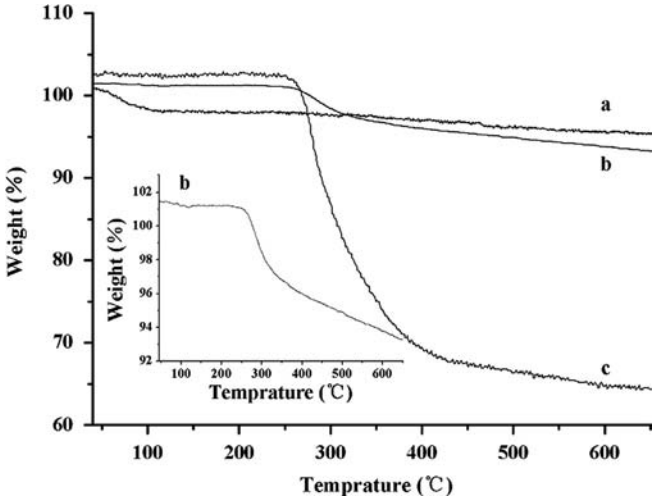

Fig. 3. TGA curves of activated silica gel particles (a), VTTS–SiO_2 (b) and MIP@SiO_2 (c).

Fig. 4 shows the SEM of silica gel and MIP@SiO_2 with different magnifications. After the growth of MIP, the surface of MIP@SiO_2 (Fig. 4d) became much coarser compared to those of the bare silica gel (Fig. 4b). The morphology of gel and MIP@SiO_2 is similar to each other as revealed in Fig. 4a and c, indicating that thickness of MIP is very thin.

The porosity of the silica particles was investigated by a nitrogen adsorption–desorption experiment (Fig. 5). Fig. 5a shows type IV curves indicating that the pore sizes of silica gel were in the mesopores range. However, Fig. 5b shows type I curves indicating that the pore sizes of MIP@SiO_2 were in the micropores range, the Brunauer–Emmett–Teller (BET) surface area obtained from the nitrogen isotherms was 100.07 $m^2 g^{-1}$, the Barret–Joyner–Halenda (BJH) pore size distribution function calculated from the adsorption branch of the isotherms showed uniform micropores with an average diameter of 0.824 nm, and the pore volume was estimated to be 0.021 $cm^3 g^{-1}$, demonstrating that the MIP layer was formed on the surface of silica gel successfully, and the entrance of mesoporous had been blocked.

3.2. *Adsorption characteristic of MIP@SiO_2*

Dynamic adsorption test was carried out at different time intervals. The adsorption kinetic curves of MEL showed an overall of two-fold increase in adsorption capacity with MIP@SiO_2 versus NIP@SiO_2 (Fig. 6), both MIP@SiO_2 and NIP@SiO_2 reached adsorption equilibrium at 10 min; however, the bulk MIP material spent 60 min to reach adsorption equilibrium due to the embedded activity site, suggesting that target molecule rebound with MIP@-SiO_2 more easily. The rapid rebinding kinetics of MEL-imprinted silica gel is attributed to the most recognition sites at the surface

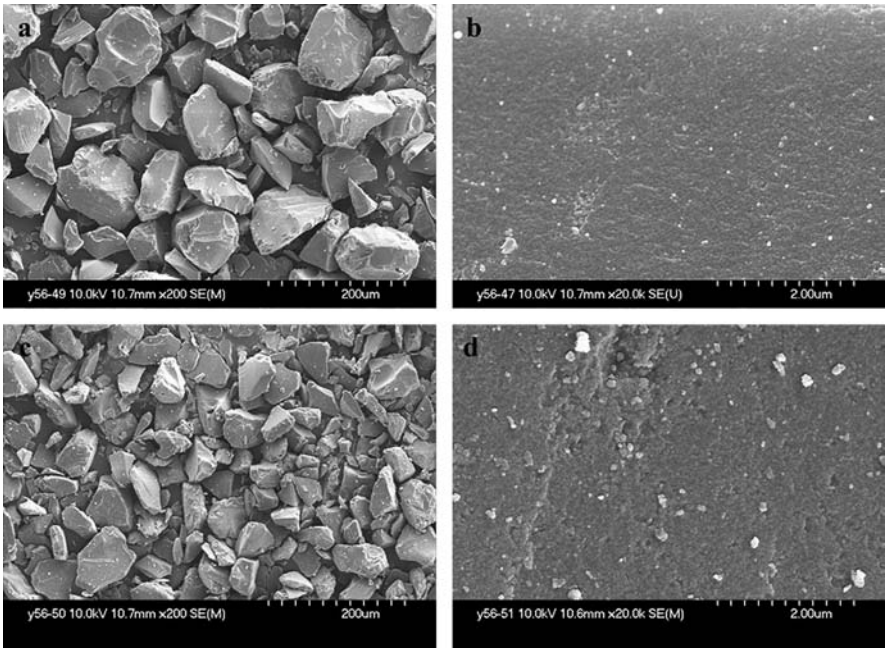

Fig. 4. SEM images of silica gel (a and b) and MIP@SiO_2 (c and d).

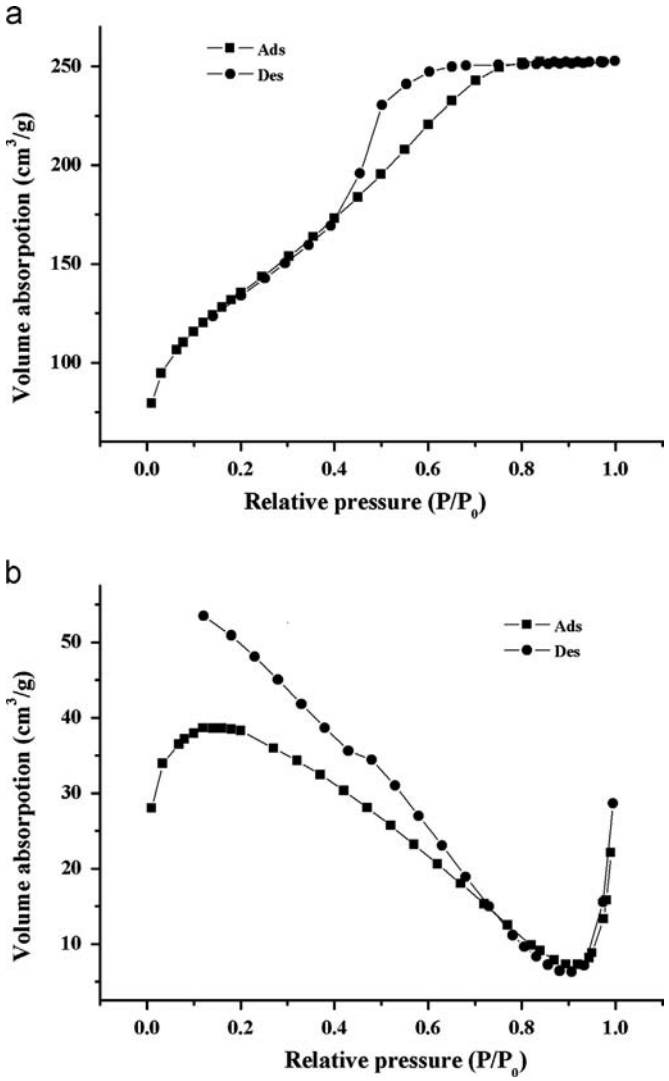

Fig. 5. N_2 adsorption and desorption isotherms of activated silica gel particles (a) and MIP@SiO_2 (b).

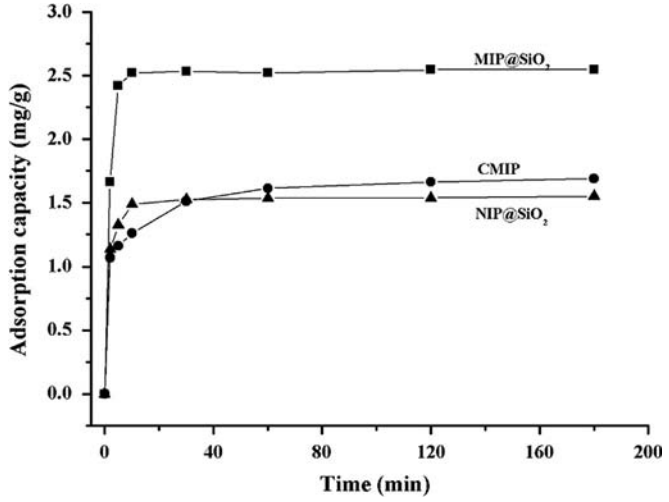

Fig. 6. Static adsorption of MEL on MIP@SiO_2, MIP and NIP@SiO_2.

or in proximity to the surface of the particles for easy diffusion of target analytes into imprinting cavities. This merit is favorable for MEL-imprinted silica used as SPE sorbent.

To measure adsorption capacity of MEL imprinted MIP@SiO_2, MEL acetonitrile solutions with different concentrations (varied from 5 to 62.5 mg L^{-1}) were prepared as extracted samples. Based on Langmuir adsorption equation, the saturated adsorption capacity of MIP@SiO_2 is 7.719 mg g^{-1}. The static adsorption capacity of MEL imprinted MIP@SiO_2 was about 22 times as much as that of reported by Yang [16]. In their research, the MEL-imprinted polymer was synthesized by bulk polymerization. This indicated the obvious dominance of MIP@SiO_2.

In general, the Scatchard plot is used for the evaluation of adsorption parameters [30]. Furthermore, the Scatchard plot can indicate how many kinds of binding sites exist in the MIPs. If the plots can be fitted into one line, it indicates that there is only one kind of binding site existing in imprinted cavities. If it can be fit into more than one line, there may be several kinds of binding sites existing. Scatchard analysis was provided by the Scatchard equation [31]. As shown in Fig. 7, the binding sites of the plot were favorably linearized into two segments. It is suggested that there are probably higher affinity site and lower affinity site with MIP@SiO_2. According to the linear regression formulas, the binding constants of $Q_{max1}=5.81$ mg g^{-1} and $K_{d1}=1.83$ g L^{-1} for higher affinity site and $Q_{max2}=2.83$ mg g^{-1} and $K_{d2}=0.51$ g L^{-1} for lower affinity site could be obtained.

3.3. Competitive selectivity of MIP@SiO_2

To evaluate the competitive selectivity of MIP@SiO_2, acetonitrile solutions of MEL/CA (Fig. 8) at three concentration levels were prepared as the extracted samples. Fig. 9 shows that the adsorption capacity of MEL is 2.55–3.67 mg g^{-1}, while the adsorption capacity of CA is only 1.23–1.79 mg g^{-1}, which indicated high discrimination property of the MIP@SiO_2 between the template and other compounds.

3.4. Stability of MIP@SiO_2

To evaluate the stability of MIP@SiO_2, the same MIP@SiO_2 was reused five times to binding/removing MEL. Repeated

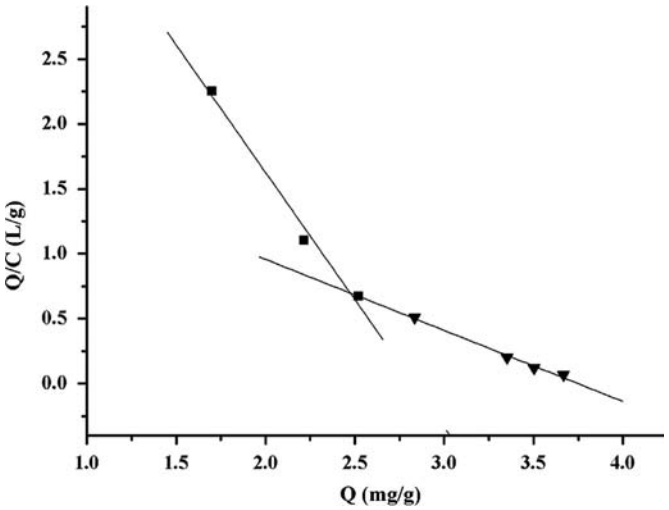

Fig. 7. Scatchard plot for MEL in MIP@SiO_2 within the range of 5–62.5 mg L^{-1}.

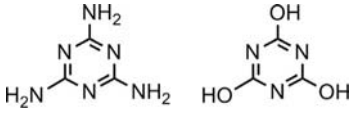

Fig. 8. Molecular structures of MEL and CA.

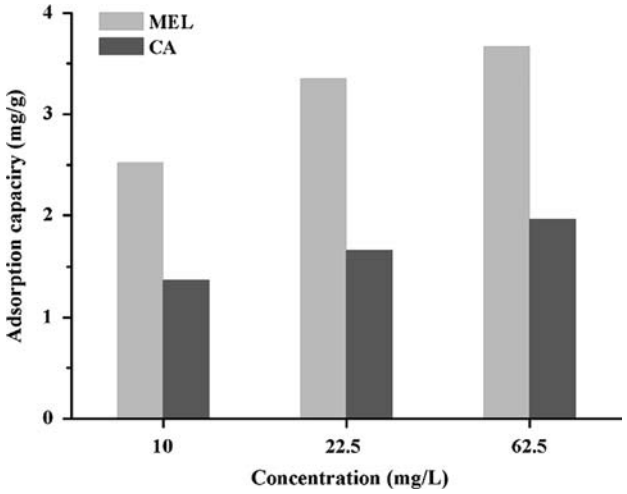

Fig. 9. Recoveries of MEL and analogs on MIP@SiO_2.

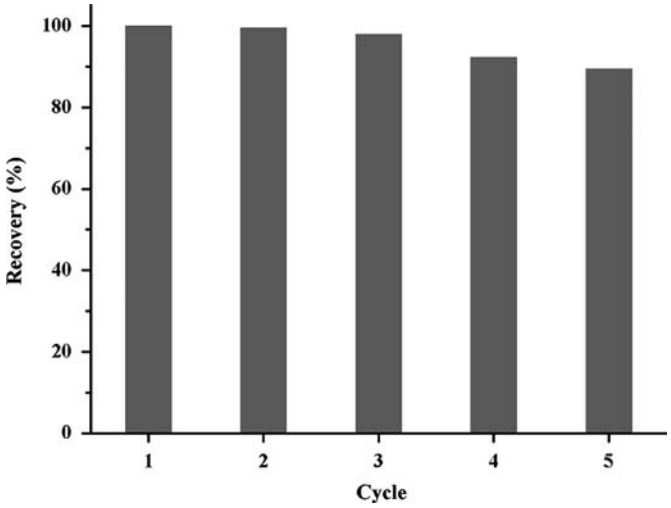

Fig. 10. Recoveries of MEL on recycling MIP@SiO_2.

Table 2
Recoveries of MEL on MI-SPE ($n=3$).

Concentration of standard solution (mg L^{-1})	Mass of MIP@SiO_2 in SPE (mg)	Recovery (%)	R.S.D. (%)
5	100	91.5	9.5
10	100	93.3	7.2

binding/removing test shows that the recovery decreased as cycle continued, but the recovery of the fifth time was still more than 90% (Fig. 10), which suggested that MIP@SiO_2 have good stability and reusability.

3.5. Evaluation of MIP@SiO_2 as SPE sorbents

The recoveries of melamine in standard solutions were calculated by 1 mL different concentration (5.0 and 10.0 mg L^{-1}) of MEL solution flow through MI-SPE. Table 2 shows that MI-SPE columns have good recoveries for melamine at different concentrations, indicating that this method could be used to detect some polluted samples.

3.6. MI-SPE for spiked milk samples

To validate the performance of MI-SPE for the bio-matrix sample, the MIP@SiO_2 and corresponding NIP@SiO_2 were packed individually into cartridges to compare their efficiency of extracting melamine from milk and milk powder. Fig. 11 shows the chromatograms of MEL in spiked milk (a) and milk powder (b), which were obtained with MI-SPE and NI-SPE, respectively. As could be observed from the chromatograms, after MI-SPE treatment, the concentration of MEL was high enough to be quantitatively analyzed while it was too low to be quantitated without SPE. As the composition of milk powder is more complex than milk samples and the ability to recognize target molecule of NIP is weaker than MIP, therefore the larger and broad peak ahead of MEL was appeared when NIP was utilized in Fig. 11(b). The peak might be other materials that extracted from milk powder by NIP through physical absorption. Moreover, the peak in the MI-SPE method was much stronger than those in the NI-SPE method of both milk and milk powder samples, indicating that MIP@SiO_2 could be used as adsorbent for SPE.

Both milk and milk powder samples were also selected for spiked analysis for validation of the method. The spiking concentrations for MEL at two levels of 2.5 and 5.0 mg L^{-1}, were subjected

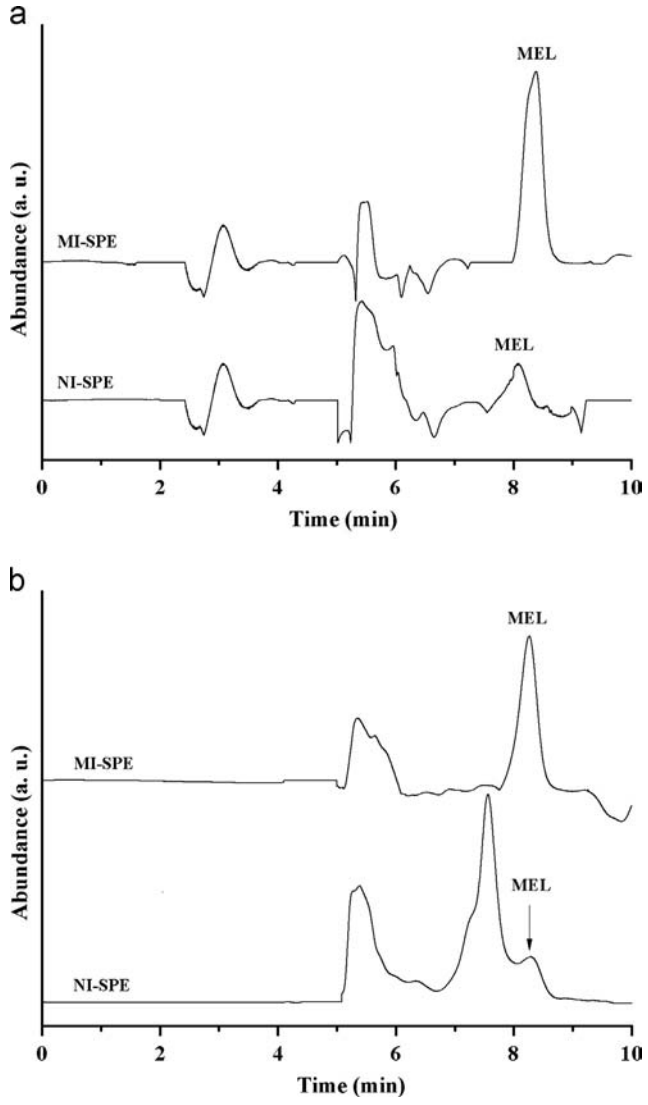

Fig. 11. HPLC chromatograms of milk (a) and milk powder (b) spiked with 2.5 mg L^{-1} MEL after extracted by MI-SPE and NI-SPE, respectively.

Table 3
Determination of MEL in milk samples ($n=3$).

Sample	MEL spiked (mg L^{-1})	Recovery (%)	R.S.D. (%)
Milk	2.5	93.5	7.8
	5.0	75.6	6.9
Milk powder	2.5	96.8	9.2
	5.0	83.5	11.4

to extraction by the MI-SPE, and then analyzed by HPLC. Table 3 shows that the recovery of spiked samples were from 75.6% to 96.8%, and the RSDs were from 6.9% to 11.4%, respectively. It could be seen that a reliable analytical method based on the MIP@SiO_2 extraction coupled with HPLC allowed the highly selective detection of MEL in complicated matrix by the proposed method.

4. Conclusion

In this study, MEL imprinted silica gel was prepared by the surface imprinting technique. When used as SPE adsorbents, these obtained MIP@SiO_2 showed high selectivity and absorption capacity, and provided fast kinetics for the rebinding of MEL. The MI-SPE showed more efficient clean-up of MEL for milk samples, indicating that the MI-SPE can be used to concentration and purification of MEL in complex matrix. Furthermore, the recoveries showed no significant decrease after the MI-SPE was reused five times, which shows that MIP@SiO_2 has good stability and reusability. Besides, the recoveries and reproducibility of the MI-SPE coupled HPLC method was acceptable. So all the results revealed that MIP@SiO_2 were efficient SPE adsorbents for MEL.

Acknowledgments

The authors thank the support from National Natural Science Foundation of China (No. 21075025) and support from Natural Science Foundation of Heilongjiang Province (No. B200910).

References

[1] B. Tomita, H. Ono, J. Polym. Sci., Part A: Polym. Chem. 17 (1979) 3205–3215.
[2] D. Frösch, C. Westphal, Electron Microsc. Rev. 2 (1989) 231–255.
[3] Y. Yang, G.J. Xiong, D.F. Yu, J. Cao, L.P. Wang, L. Xu, R.R. Mao, Toxicol. Lett. 214 (2012) 63–68.
[4] G.G. da Costa, C.C. Jacob, L.S. Von Tungeln, N.R. Hasbrouck, G.R. Olson, D.G. Hattan, R. Reimschuessel, F.A. Beland, Toxicol. Appl. Pharmacol. 262 (2012) 99–106.
[5] H. Sun, L. Wang, L. Ai, S. Liang, H. Wu, Food Control 21 (2010) 686–691.
[6] N. Yan, L. Zhou, Z. Zhu, X. Chen, J. Agric. Food Chem. 57 (2009) 807–811.
[7] M.S. Filigenzi, E.R. Tor, R.H. Poppenga, L.A. Aston, B. Puschner, Rapid Commun. Mass Spectrom. 21 (2007) 4027–4032.
[8] R. Wei, R. Wang, Q. Zeng, M. Chen, T. Liu, J. Chromatogr. Sci. 47 (2009) 581–584.
[9] Y.T. Wu, C.M. Huang, C.C. Lin, W.A. Ho, L.C. Lin, T.F. Chiu, D.C. Tarng, C.H. Lin, T.H. Tsai, J. Chromatogr. A. 1216 (2009) 7595–7601.
[10] L. Meng, G. Shen, X. Hou, L. Wang, Chromatographia 70 (2009) 991–994.
[11] X.J. Deng, D.H. Guo, S.Z. Zhao, L. Han, Y.G. Sheng, X.H. Yi, Y. Zhou, T. Peng, J. Chromatogr. B 878 (2010) 2839–2844.
[12] Z.C. Zhang, Z.Q. Cheng, C.F. Zhang, H.Y. Wang, J.F. Li, J. Appl. Polym. Sci. 123 (2012) 962–967.
[13] B. Wang, Y.Z. Wang, H. Yang, J.Q. Wang, A.P. Deng, Microchim. Acta 174 (2011) 191–199.
[14] W.H. Yang, S.L. Yan, C. Wei, Q.Z. Wang, Acta Polym. Sin. (2010) 1163–1169.
[15] M. Curcio, F. Puoci, G. Cirillo, F. Iemma, U.G. Spizzirri, N. Picci, J. Agric. Food Chem. 58 (2010) 11883–11887.
[16] H.H. Yang, W.H. Zhou, X.C. Guo, F.R. Chen, H.Q. Zhao, L.M. Lin, X.R. Wang, Talanta 80 (2009) 821–825.
[17] R. Zhu, W. Zhao, M. Zhai, F. Wei, Z. Cai, N. Sheng, Q. Hu, Anal. Chim. Acta 658 (2010) 209–216.
[18] L.M. He, Y.J. Su, Y.Q. Zheng, X.H. Huang, L. Wu, Y.H. Liu, Z.L. Zeng, Z.L. Chen, J. Chromatogr. A 1216 (2009) 6196–6203.
[19] V. Pichon, F. Chapuis-Hugon, Anal. Chim. Acta 622 (2008) 48–61.
[20] V. Pichon, J. Chromatogr. A 1152 (2007) 41–53.
[21] L.M. He, Y.J. Su, X.G. Shen, Y.Q. Zheng, H.B. Guo, Z.L. Zeng, J. Sep. Sci. 32 (2009) 3310–3318.
[22] Z.C. Lin, W.J. Cheng, Y.Y. Li, Z.R. Liu, X.P. Chen, C.J. Huang, Anal. Chim. Acta 720 (2012) 71–76.
[23] F.T.C. Moreira, R.A.F. Dutra, J.P.C. Noronha, M.G.F. Sales, Biosens. Bioelectron. 26 (2011) 4760–4766.
[24] F. Deng, Y. Li, X. Luo, L. Yang, X. Tu, Colloid Surf. A Physicochem. Eng. Aspect 395 (2012) 183–189.
[25] S. Balamurugan, D.A. Spivak, J. Mol. Recognition 24 (2011) 915–929.
[26] J. Gauczinski, Z. Liu, X. Zhang, M. Schönhoff, Langmuir 28 (2012) 4267–4273.
[27] H. Xu, M. Schönhoff, X. Zhang, Small 8 (2012) 517–523.
[28] A.R. Sarkar, P.K. Datta, M. Sarkar, Talanta 43 (1996) 1857–1862.
[29] Y. Ji, J. Yin, Z. Xu, C. Zhao, H. Huang, H. Zhang, C. Wang, Anal. Bioanal. Chem. 395 (2009) 1125–1133.
[30] J. Ma, L. Yuan, M. Ding, S. Wang, F. Ren, J. Zhang, S. Du, F. Li, X. Zhou, Biosens. Bioelectron. 26 (2011) 2791–2795.
[31] Y. Zhang, Y. Li, Y. Hu, G. Li, Y. Chen, J. Chromatogr. A 1217 (2010) 7337–7344.